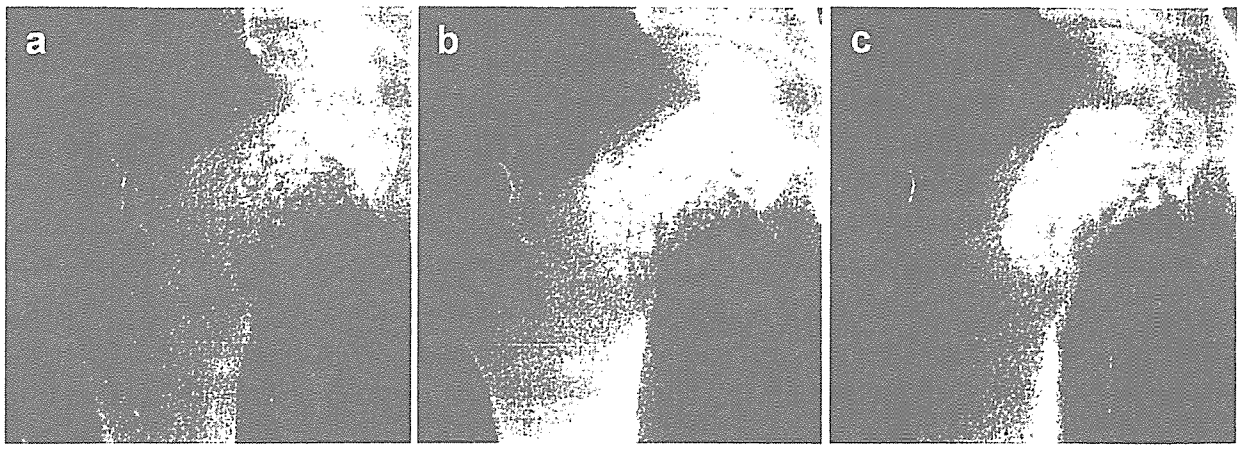

図2　ネオボーン®移植後のX線経過．18歳女性，大腿骨頚部骨巨細胞腫．(a)手術直後のX線像．(b)移植後2カ月でわずかに移植部のX線透過性が低下し，(c)6カ月では顆粒が融合し強い硬化像を示している．

侵入は良好で，6週間で円柱の中心部，すなわち表層から3 mmまでほぼすべての気孔内に成熟骨組織の侵入が見られたが，IP-CHA69では6週で表層から2 mmまでの気孔内にしか骨形成が見られず，中心部の深さ3 mmでは線維性結合織のみが形成されており，気孔率を下げると気孔内への骨組織侵入の速度が低下した．既製の多孔体HA骨補填材でも6週の時点で中心部の深さ3 mmではほとんど骨形成が見られなかった．IP-CHA75の初期強度は10-12 MPaであるが，骨内埋植後，インプラント中心部分の圧縮強度を計測すると，骨形成が進むにつれて上昇し，埋植後6週で20 MPa，9週で30 MPa以上の圧縮強度に達しており，移植後速やかに強度を獲得する．これらのことから，臨床で用いるには気孔率75%，気孔径150-200 μm，平均気孔間連通孔径40 μmのものが至適と考え骨補填材として臨床用に開発した．

IP-CHA/ネオボーン®の臨床的特徴

IP-CHA75/ネオボーン®を骨補填材として開発するにあたり行った臨床治験の結果[10]では，良性骨腫瘍および腫瘍類似疾患の手術において使用した場合，単純X線上，術後2-3カ月でネオボーン®移植部の骨硬化が出現し，6カ月ではほぼすべての症例で強い骨硬化に伴いネオボーン®顆粒間や骨との間が不明瞭になるという変化が観察された(図2)．このようなX線変化は従来の多孔体HA人工骨では通常平均術後12カ月ごろで見られるとされており，ネオボーン®のX線上の変化はきわめて速いと考えられるが，これはネオボーン®では顆粒間だけでなく気孔の内部にも骨形成が起こるためと考えられる．また，このようにX線上早期から硬化像が明らかとなることは，臨床医にとって荷重開始可能時期を推測するのに好都合である．強度については，手術中の操作には問題がなく，エアートームなどによる加工も容易であるが，ハンマーなどで衝撃を加えれば破損する．荷重部など強い力学的負荷のかかる部位での単独使用は難しく，適宜，金属製プレートなどの併用が必要である．

ネオボーン®の特徴を生かした適応拡大の試み

この20年間に種々のリン酸カルシウム系骨補填材が製品化されてきたが，臨床医にとっては選択肢が増え，歓迎すべきである一方，それぞれの製品の特徴をよく理解し，個々の症例の病態に合わせて正しい材料を選択することが要求される．たとえば，オスフェリオン®(オリンパス光学製)は，初期強度が低いものの，吸収されやすく自家骨に置換されやすい特徴を生かして，小児や関節軟骨下骨部の骨欠損に有利と考えられる．セメントのように硬化するリン酸カルシウムペーストのバイオペックス®(三菱マテリアル製)は，その操作性が魅力であるが，十分な強度を得るには操作に熟練を要するとともに，bone ingrowthは期待できないため，小皮切による低侵襲手術や上肢など非荷重部での使用に向いている．

ネオボーン®についても，その特性を理解し，適所に用いることが肝要である．既製の骨補填材と比較したネオボーン®の特徴は，①臨床的に速やかに移植部の骨と融合する，②深部気孔内骨組織侵入(bone ingrowth)が期待できる(ブロック体や特殊形状のインプラントを含めて)，③術前，術中の加工が容易である，④吸収はきわめて緩徐か，または吸収されない，⑤強

度は海綿骨の数倍程度で荷重部での単独使用には不十分，⑥連通気孔構造のため，深部気孔内への細胞の導入が容易である，といったことが挙げられる．これらの特性を理解した上で，われわれが積極的にネオボーン®を使用しているのが，これまで人工骨があまり適用されず自家骨が主として用いられてきた楔状矯正骨切り術[11),12)]，関節リウマチ(rheumatoid arthritis: RA)を中心とする母床骨の状態が悪い疾患での手術(関節固定術や大きな軟骨下嚢腫を伴うTKA〈total knee arthroplasty〉など)，偽関節手術(自家骨と併用または単独で)[13)]などである．これらの領域では現在も自家骨移植が標準的治療であるが，自家骨移植のために，腸骨などから移植片を採取する手技は余分な術創を作るだけでなく，出血および手術時間を増大し，術後の執拗な痛み，骨折，神経損傷など合併症を高率に引き起こすことが知られており[14),15),16)]，代用できる場合はできるだけ人工骨を用いるべきである．また自家骨を移植片として用いる楔開き矯正骨切り術では，術中に加工を行う必要があるため正確な移植片を得ることが困難である．ネオボーン®の場合，患部の術前CT(computed tomography)データなどに基づいて術前に正確な移植片の作成が可能であり，海綿骨の数倍の圧縮強度を有し，さらにブロック体でもbone ingrowthが期待できることから，矯正骨切り術において有用性が高いと考えている[11),12)]．図3-a，b，cは48歳女性，橈骨遠位端骨折の保存的治療後の変形治癒であるが，術前のCTから再構成した三次元画像において，楔開き骨切り術のシミュレーションを行い，楔状の移植片の形状を決定した．この形状の三次元データに基づき，切削ラピッドプロトタイピング(RP)の手法を用いて，ネオボーン®の直方体ブロックから移植用の楔状ブロック体を削り出した．近年の工業製品はCAD(computer-aided designing)すなわちコンピューター上でデザインされるが，切削RPとはその試作品を，三次元CADデータを元にコンピューター制御でプラスチックなどをドリルで削って作成する方法である．この方法で作成した楔状ブロックは，術中一切加工せずに骨切り部にフィットし正確な矯正が得られた．10カ月後のX線像では移植したブロックの圧潰はなく矯正位が保たれ，完全な骨癒合が得られていた．

RAの骨は骨粗鬆化が強いため，人工関節置換術や関節固定術を行う場合，手術部位の骨の脆弱性や骨欠損が問題となるだけでなく，自家骨移植のための採骨部でも同様で質のよい移植骨を大量に採取することは困難である．また，RAの患者はしばしば繰り返し多数の手術を必要とするため，むやみに自家骨を大量採取することは避ける必要がある．図3-d，eはそれぞれ77歳女性の距骨下関節破壊，および60歳女性のRAの手関節，母指MP関節破壊に対し，ネオボーン®顆粒を使用して関節固定術を行った例である．ネオボーン®はこのようなRAの関節固定においてもよく母床骨と一体化し，かつ吸収性が低いため，長期にわたって安定した固定が得られる．また骨破壊が強いRAや関節直下の嚢胞性変化により大きな骨欠損を伴うRAに対する人工関節置換術においても，われわれは骨欠損の補填に，ネオボーン®を局所で得られる自家骨に併用して用いている．

骨折遷延治癒の標準的治療は自家骨移植であるが，ここでも自家骨の小片にネオボーン®の顆粒を混ぜて使用することにより，自家骨の使用量が減らせる利点がある[13)]．図3-f，g，hは36歳男性の下腿骨開放骨折後遷延治癒の症例であるが，自家腸骨より得た海綿骨小片とネオボーン®顆粒を混合し，偽関節部分の骨内外に移植したところ，良好な骨形成が起こり，術後約1年で創外固定を除去し，全荷重歩行が可能となった．このようにわれわれはネオボーン®の特徴を利用してこれまで人工骨が敬遠されていた領域で，ネオボーン®単独または自家骨と併用での使用を試みており，症例数はまだ少ないが良好な印象を得ている[9)]．

骨再生医療のscaffoldとしての有用性

もう1つの新たな試みは，再生医療への応用である．IP-CHAの連通性に優れた気孔には，血管や新生骨など再生に必要な組織の侵入が容易なだけでなく，液体に浮遊させた細胞や骨形成因子(bone morphogenetic protein: BMP)溶液の導入が容易であり，骨の再生医療における間葉系幹細胞やBMPなどの“足場(scaffold)”として有用であると考えられる．これまでにわれわれは，基礎実験において間葉系幹細胞を用いた系[17)]やBMPを用いた系[18),19)]でその有用性を証明してきた．これらの実験結果を得て，われわれは大阪大学医学部附属病院未来医療センターの臨床研究プロジェクトとして，良性骨腫瘍および骨腫瘍類似疾患の患者を対象に，「自家骨髄由来培養細胞導入人工骨による骨疾患の治療」を開始している．局麻下に骨髄穿刺を行い，患者腸骨より15-50 mlの骨髄液を得る．骨髄細胞を，15%自己血清を含むαMEM培地で2-3週間ほど培養すると，紡錘形の付着性細胞が増殖してくる．この細胞

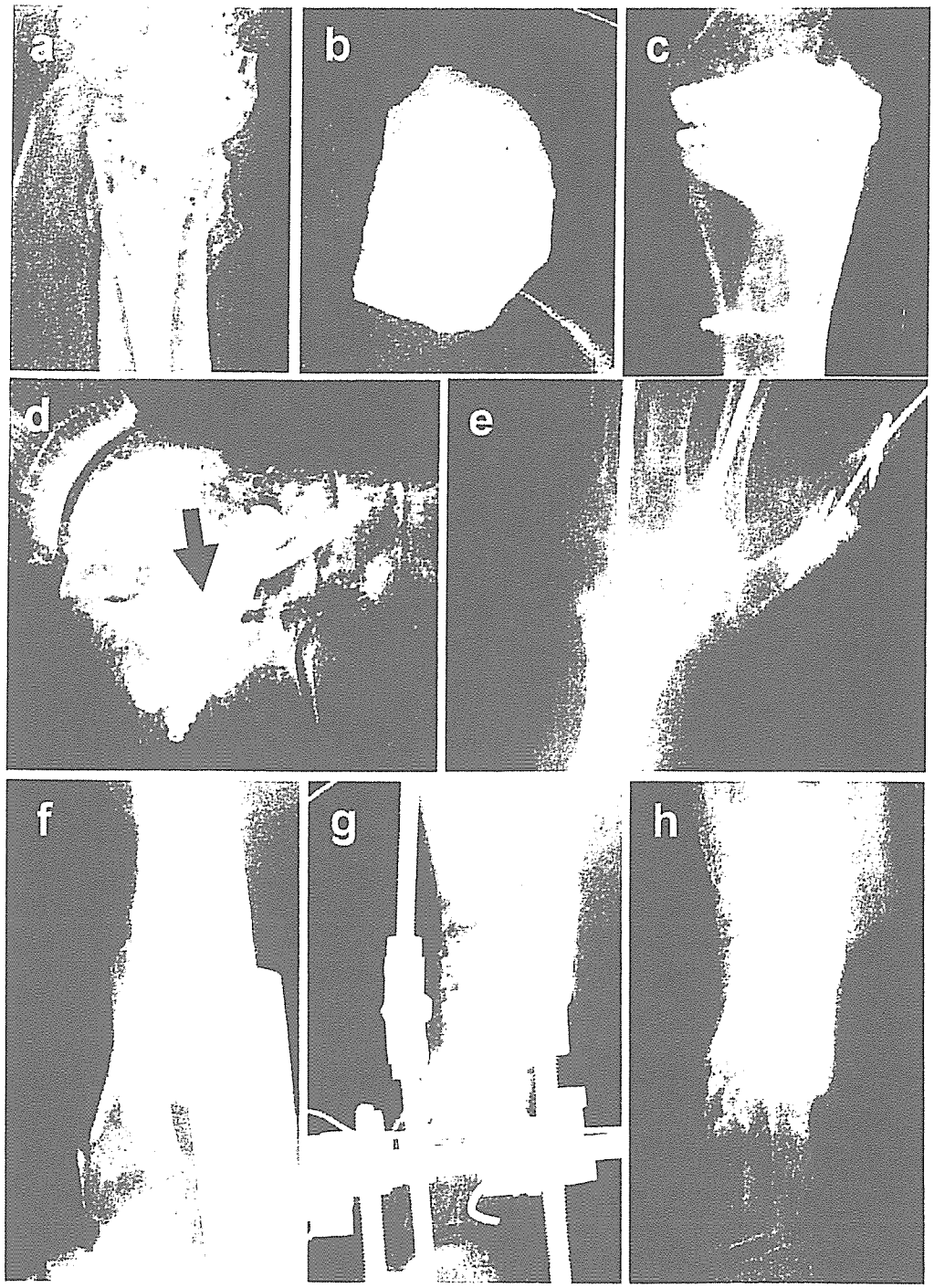

図3　ネオボーン®の臨床応用.

(a), (b), (c)　48歳女性，橈骨遠位端骨折変形治癒に対する楔開き矯正骨切り術．(a)術前の単純X線側面で背屈変形を認める．(b)切削ラピッドプロトタイピングの手法を用いて作成した楔状スペーサー．(c)正確な矯正が得られ，術後10カ月のX線では完全な骨癒合が得られている．

(d), (e)　関節リウマチに対する関節固定術．(d)77歳女性，自家骨を用いず距骨下関節固定術を施行，術後7カ月で良好な固定が得られている．(e)60歳女性，ネオボーン®単独で手関節および母指MP関節固定術を行った．術後3年のX線像でもネオボーン®の吸収はほとんど見られず，安定した固定が保たれている．

(f), (g), (h)　36歳男性，下腿骨開放骨折後遷延治癒の症例．(f)初期治療として創外固定が行われたが遷延治癒となった．(g)自家腸骨より得た海綿骨小片とネオボーン®顆粒を混合し，偽関節部分の骨内外に移植した．(h)良好な骨形成が起こり，術後約1年で創外固定を除去し，全荷重歩行が可能となった．

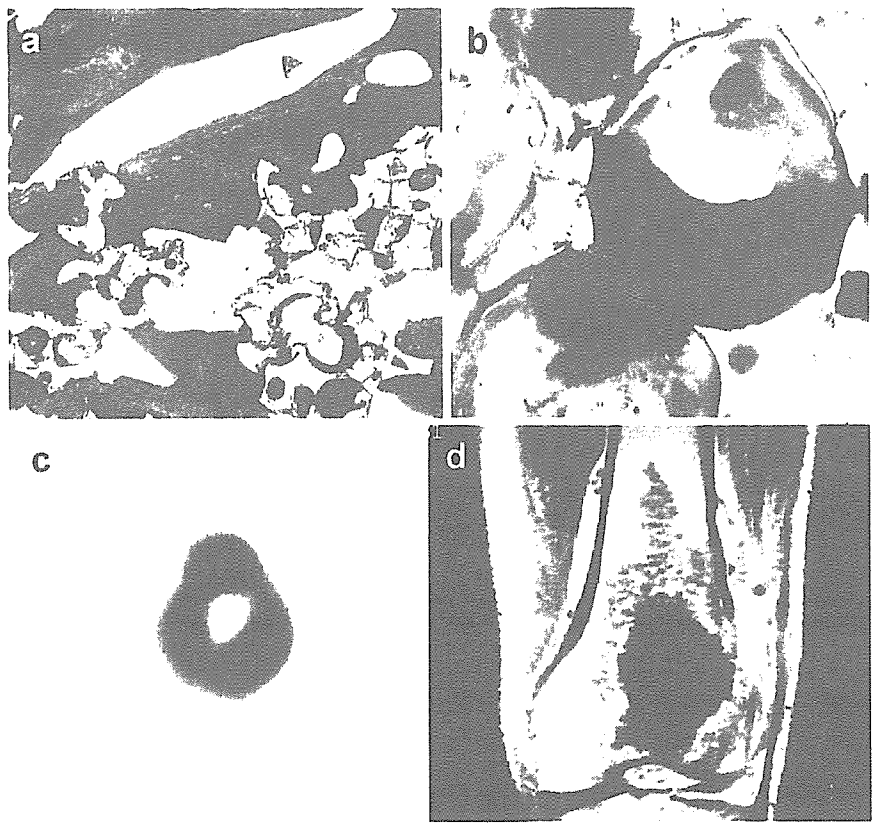

図4 臨床例における骨形成の評価.
(a), (b) ネオボーン®移植後7カ月，抜釘時に得られた組織の非脱灰硬組織切片トルイジンブルー染色像では顆粒の周辺(a)，および気孔内(b)に豊富な新生骨が観察される.
(c), (d) ネオボーン®移植後，2カ月での画像評価. (c) ^{99m}Tc-MDPによる骨シンチのSPECT像では，ネオボーン®移植部の周辺部にリング状の取り込みが見られ，周辺部から骨形成が始まっているのがわかる. (d)造影MRIにおいても，周辺部がリング状に造影され，周辺部から血液供給が再開している.

は約90%が増殖能と骨芽細胞など間葉系細胞への分化能を維持する間葉系幹細胞である. この細胞の浮遊液に，ネオボーン®を1晩浸すと気孔内に細胞が導入され気孔壁に付着する. これをさらに約2週間，アスコルビン酸，β-グリセロリン酸，デキサメサゾンを添加した15%自己血清を含むαMEMで培養し骨芽細胞へ分化誘導したのち，手術で骨欠損部に移植している. この方法は将来的には，骨形成にとってきわめて不利な条件の病巣，たとえば悪性腫瘍切除後や外傷，骨髄炎などによる巨大な骨欠損を機能的に再建するための新しい治療法として期待している.

気孔内骨形成の臨床評価－ヒトでも気孔内骨形成は起こっているか？

先に述べたように，動物実験ではブロック体においても良好な気孔内への新生骨侵入が確認されているが，ヒトの臨床例における気孔内骨侵入は評価が困難である. これまでに少数の症例で抜釘時や再手術時にネオボーン®移植部の一部の組織が得られており，顆粒周囲や気孔内に新生骨が形成されている像が得られている(図4-a, b)が，実際にどれだけの範囲に骨形成が起こっているのかは，小さな生検材料による組織学的検討では知ることができない. 患者の経過観察中に人工骨移植部の骨形成の状態をその範囲を含めて低侵襲的に判定する方法として，われわれは^{99m}Tc-MDP SPECTおよびガドリニウム造影MRIに注目している(図4-c, d). 造影MRIでは，大腿骨近位の骨腫瘍に対しネオボーン®顆粒充填後，10カ月程度で充填部全領域が造影されるようになり，血行が再開していた[20]. このMRIで造影される領域が，骨形成が起こっている領域と一致するかどうかは今後の検討を要する.

ま と め

IP-CHA/ネオボーン®は，骨補填材としてこれまで臨床現場で実績を積み重ねてきた多孔体HA人工骨の三次元的気孔構造を制御することにより改良した新しい多孔体人工骨である．その最大の特徴は，気孔が細胞や組織が通過するのに十分な大きさの気孔間連通孔で連続していることであり，それと同時に臨床的に骨補填材として使用可能な強度を有している．経時的X線変化で評価した移植部の骨形成は従来の多孔体HA人工骨に比べ速やかであり，これまでに自家骨移植が標準的治療で人工骨が使われなかった領域にまで適応できる可能性をもつ．また，ネオボーン®が骨再生のscaffoldとして応用できる可能性を臨床試験で検討している．このような人工骨の適応拡大や骨再生医療の発展は，自家骨採取を最小限に減らすことにつながり，また将来的に難治性・大型骨欠損に対するより機能的な再建を可能にすると考えられる．

物質・材料研究機構生体材料研究センター 田中順三主任研究員，菊池正紀研究員，生駒俊之研究員，国立病院機構相模原病院 越智隆弘院長，産業技術総合研究所セルエンジニアリング研究部門 大串始先生，大阪市立大学整形外科高岡邦夫教授をはじめ，本研究にご協力・ご指導いただいた多くの先生方に深謝いたします．

文　献

1) Ayers RA, Simske SJ, Nunes CR, et al. Long-term bone ingrowth and residual microhardness of porous block hydroxyapatite implants in humans. J Oral Maxillofac Surg 1998; 56: 1297-301.
2) 日比敦夫，石川忠也，浅野昌育他．良性骨腫瘍に対するハイドロキシアパタイト充填後の成績不良例についての検討．整形外科 1994; 45: 1423-8.
3) Kamegaya M, Shinohara Y, Shinada Y, et al. The use of a hydroxyapatite block for innominate osteotomy. J Bone Joint Surg Br 1994; 76: 123-6.
4) Uchida A, Araki N, Shinto Y, et al. The use of calcium hydroxyapatite ceramic in bone tumor surgery. J Bone Joint Surg Br 1990; 72: 298-302.
5) 吉田行雄，松井宣夫，大塚隆信．骨腫瘍および腫瘍類似疾患に対する合成水酸化アパタイトの長期成績．関節外科 1995; 14: 1379-85.
6) Matsumine A, Myoui A, Kusuzaki K, et al. Calcium hydroxyapatite ceramic implants in bone tumor surgery. A long-term follow-up study. J Bone Joint Surg Br 2004; 86: 719-25.
7) Yoshikawa H, Uchida A. Clinical application of calcium hydroxyapatite ceramic in bone tumor surgery. In: Wise DL, editor. Biomaterials and bioengineering handbook. New York: Marcel Dekker; 2000. p.433-55.
8) Tamai N, Myoui A, Tomita T, et al. Novel hydroxyapatite ceramics with an interconnective porous structure exhibit superior osteoconduction in vivo. J Biomed Mater Res 2001; 59: 110-7.
9) Myoui A. Three-dimensionally engineered hydroxyapatite ceramics with interconnected pores as a bone substitute and tissue engineering scaffold. In: Yaszemski MJ, Trantolo DJ, Lewandrowski K, et al, editors. Biomaterials in orthopedics. New York: Marcel Dekker; 2003. p287-300.
10) 名井陽，古野雅彦，荒木信人他．連通気孔を有する新規ハイドロキシアパタイトセラミックスの優れた骨伝導能．臨床整形外科 2001; 36: 1381-8.
11) 村瀬剛，森友寿夫，後藤晃他．肘過伸展外反変形に対して3Dコンピューターシミュレーションを用いて尺骨矯正骨切り術を行った一例．日本肘関節学会雑誌 2004; 11: 53-4.
12) 村瀬剛，海渡貴司，名井陽他．CTデータに基づく3D-CADを利用したハイドロキシアパタイトインプラントの術前モデリング．日整会誌 2005; 79: S205.
13) 中瀬尚長，藤井昌一，早石泰久他．開放骨折後の骨欠損に対する新規ハイドロキシアパタイトセラミックスの使用効果．別冊整形外科【骨・軟骨移植最近の知見】2005; 47: 192-8.
14) Arrington ED, Smith WJ, Chambers HG, et al. Complications of iliac crest bone graft harvesting. Clin Orthop 1996; 329: 300-9.
15) Banwart JC, Asher MA, Hassanein RS. Iliac crest bone graft harvest donor site morbidity. A statistical evaluation. Spine 1995; 20: 1055-60.
16) Younger EM, Chapman MW. Morbidity at bone graft donor sites. J Orthop Trauma 1989; 3: 192-5.
17) Nishikawa M, Myoui A, Ohgushi H, et al. Bone tissue engineering using novel interconnected porous hydroxyapatite ceramics combined with marrow mesenchymal cells: Quantitative and three-dimensional image analysis/ceramic construct: comparison with marrow mesenchymal cell/ceramic composite. Cell Transplant 2004; 13: 367-76.
18) Kaito T, Myoui A, Takaoka K, et al. Potentiation of the activity of bone morphogenetic protein-2 in bone regeneration by

a PLA-PEG/hydroxyapatite composite. Biomaterials 2005; 26: 73-9.
19) Akita S, Tamai N, Myoui A, et al. Capillary vessel network integration by inserting a vascular pedicle enhances bone formation in tissue-engineered bone using interconnected porous hydroxyapatite ceramics. Tissue Eng 2004; 10: 789-95.
20) 中紀文, 荒木信人, 橋本伸之他. 造影 MRI を用いた人工骨内への血管侵入度評価. 日整会誌 2005; 79: S580.

Dual Hydroxyapatite Composite With Porous and Solid Parts: Experimental Study Using Canine Lumbar Interbody Fusion Model

Takashi Kaito, Yoshihiro Mukai, Masataka Nishikawa, Wataru Ando, Hideki Yoshikawa, Akira Myoui

Department of Orthopaedics, Osaka University Graduate School of Medicine, 2–2 Yamadaoka, Suita, Osaka 565-0871, Japan

Received 23 March 2005; revised 30 August 200; accepted 12 October 2005
Published online 30 January 2006 in Wiley InterScience (www.interscience.wiley.com). DOI: 10.1002/jbm.b.30498

Abstract: Hydroxyapatite (HA) has been evaluated for use in a variety of applications in bone reconstruction surgery because of its high affinity with host bone and biocompatibility. However, because of the difficulty in combining porosity (for bone ingrowth) and strength in HA, it is generally considered inappropriate to use HA for high-load applications such as spinal interbody fusion. In the present study, we constructed a HA implant for spinal interbody fusion, composed of a dual HA composite (DHC) that combines two HA materials with different porosities: HA with 75% porosity, for bone ingrowth; and HA with 0% porosity, for load bearing. We used a canine lumbar interbody fusion model to evaluate bone conduction of the implant and its efficacy for bony fusion. Six months after the operation, DHC exhibited almost the same efficacy for bony fusion as iliac bone grafts. Moreover, pores of the porous part of the DHC were completely filled with newly formed bone and bone marrow cells. The present findings indicate that DHC is suitable for use as an implant material for spinal interbody fusion as a substitute for iliac bone grafts, which could eliminate the disadvantages associated with autograft harvesting. © 2006 Wiley Periodicals, Inc. J Biomed Mater Res Part B: Appl Biomater 78B: 378–384, 2006

Keywords: hydroxyapatite; spinal fusion; composite

INTRODUCTION

When instability of the spine causes persistent local pain or neurological impairment, it is often treated by fusion of the affected vertebral motor segments with autologous bone graft by itself or in combination with carbon or titanium cage.[1–3] So at this point, autologous bone graft from the iliac crest is the gold standard material for spinal fusion, despite disadvantages such as limited supplies of suitable bone, cosmetic damage at the donor site, and persistence of pain, nerve damage, and fracture. Allografting is not associated with donor site problems, but it involves risks of disease transmission and immunological reaction.[4] Hydroxyapatite (HA) implants are an attractive alternative to bone grafts for use in spinal arthrodesis. Porous ceramics provide a three-dimensional (3D) scaffold for the osteoconductive latticework that is necessary for host ingrowth. HA can chemically bond with host bone, and studies clearly indicate that it is a biocompatible material.[5,6] However, the difficulty in striking a balance between porosity (for bone ingrowth) and strength has prevented widespread use of HA as an implant material for use in spinal interbody fusion.[7–11] To address this problem, we synthesized a dual HA composite (DHC) consisting of a core of HA with 75% porosity (for bone ingrowth) surrounded by solid HA with 0% porosity (for load bearing). The porous part of the composite is a material that we previously reported as interconnected porous calcium HA ceramic (IP-CHA). This porous material is synthesized using a unique "foam–gel" technique that produces its distinctive, uniform porous structure.[12]

In the present study, we used an anterior interbody fusion model of the canine lumbar spine to assess the efficacy of DHC as a spinal interbody fusion implant, compared with iliac bone grafts, in terms of bony fusion.

MATERIALS AND METHODS

Design of Implants

The implants were designed to fit the canine intervertebral space (Figure 1). Also, a stainless steel plate, with four screw holes for internal fixation, was designed to fit the canine spine (Figure 1).

Preparation of Implants

Hexagonal prisms of DHC were obtained from Toshiba Ceramics (Kanagawa, Japan) (Figure 1). The DHC consisted of

Correspondence to: T. Kaito (e-mail: t-kaito@feto.comet.ne.jp)
Contract grant sponsor: Ministry of Health, Labor and Welfare, Japan
Contract grant sponsor: Ministry of Education, Culture, Sports, Science and Technology, Japan; contract grant number: 15209050

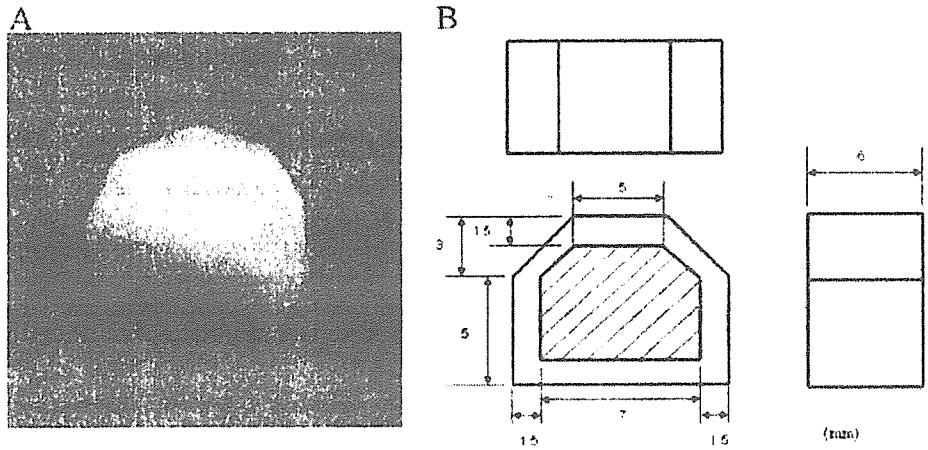

Figure 1. Macroscopic view (A) and dimensions (B) of dual hydroxyapatite composite (DHC) implant for canine intervertebral body fusion. Hatched area represents porous part (75% porosity).

two forms of HA with different porosity. A porous HA ceramic core with 75% porosity was surrounded by a solid HA ceramic with 0% porosity. The material comprising the porous HA ceramic core was IP-CHA, which has a uniform interconnected porous structure with an average interconnection channel diameter of 40 μm. Theoretically, more than 90% of the pores are connected to each other by channels with a diameter greater than 10 μm, allowing tissue to spread from pore to pore.[12] Briefly, the method used to produce DHC is as follows:

1. *Preparation of Porous HA Ceramic:*

A slurry containing HA (60 wt %) and a crosslinking substrate (polyethyleneimine, 40 wt %) was mixed with a foaming agent (polyoxyethylene lauryl ether, 1 wt %). Then, the slurry was gelatinized by adding another crosslinking agent (poly-functional epoxy compound). After the gelatinization, a hexagonal prism was carved out of the porous gel.

2. *Preparation of Solid HA Ceramic:*

A piece of the carved porous gel was placed in the center of a hexagonal mold with larger dimensions. A slurry with the same composition as the above-mentioned slurry, but lacking the foaming agent, was mixed with the gelatinization agent and poured into the mold so that it surrounds the porous gel. The nonfoaming slurry infiltrated the surface layer of the porous part and then hardened to form the solid HA ceramic, such that the solid and porous parts of the composite were tightly bound together. Then, the dual composite was removed from the mold, dried, and sintered at 1200° C.

Mechanical Compression Test

Compression tests were performed using AUTOGRAPH AG-10KNI (Shimadzu Corp., Kyoto, Japan), with a compression speed of 1 mm/min. Compression load was applied separately to the porous and solid parts, and the compressive strength was determined. Maximum breaking load of the hexagonal DHC implant was measured by applying a vertical compressive load to the specimen, across the hexagonal surface plane (N = 4). All data were expressed as the average value ± standard error.

Animal Experiment

Eight adult, female, pure-bred beagles aged ~1.5 years and weighing 12–14 kg underwent surgical opening of a left retroperitoneal approach to the lumbar spine. The surgery was performed using general anesthesia, aseptic conditions, and perioperative antibiotics. The segmental vessels of L2 and L3 were coagulated and transected to expose the bodies of L2 and L3. Then, the center portion of the intervertebral disc was identified and evacuated including the adjacent endplates of L2 and L3, using steel and diamond burrs to expose bleeding subchondral bone. The defect size was adjusted using a metal trial tool that was the same size as the implant. We then performed one-level arthrodesis by placing an iliac bone graft (IBG group) or a DHC graft (DHC group) in the defect. In all animals, internal fixation was achieved using a plate and four cortical screws (ϕ, 4.0 mm) (Figure 2). The animals were allowed unrestricted activity after the operative procedure, and were kept in accordance with our institutional guidelines for care and use of laboratory animals. Dogs were killed by overdose anesthesia, and the spine segment from L1 to L4 was harvested 6 months after operation. Then, the internal fixators were removed. All procedures involving animals were approved by the Animal Care and Use Committee of Shin Nippon Biomedical Laboratories and performed in accordance with standards published by the National Research Council.

Radiographic Examination

All harvested tissues were fixed with 10% neutral formalin, and were then radiographed with a soft X-ray apparatus (M-60, SOFTEX Corp., Ebina, Japan) and micro-focus CT scanning apparatus (SMX-100CT, SHIMADZU, Kyoto, Japan). On radiographs and CT images, fusion was defined as

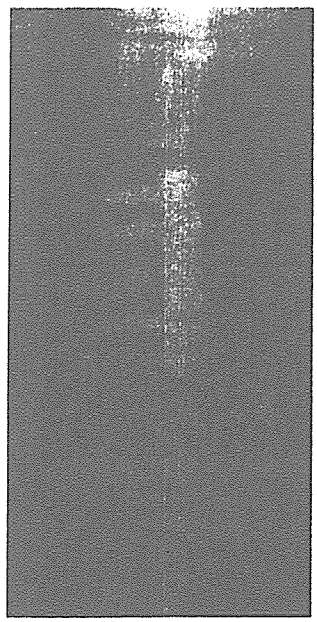

Figure 2. Postoperative A-P radiographic view of canine lumbar spine.

a continuous trabecular bone bridge across the inner part of the implant, with no obvious interruption by a radiolucent line.

Histological Evaluation

All tissue samples harvested together with the neighboring vertebral bone from each group were demineralized with 50% formic acid and 10% sodium citrate, dehydrated through an ethanol series and embedded in paraffin wax. Sections (thickness, 5 μm) were cut, stained with hematoxylin and eosin, and examined under a light microscope.

Bony union was quantified by calculating % length of bony fusion, which is judged by bridging trabecular bone between host bone and porous part of DHC or iliac bone graft histomorphometrically. Solid parts of DHC were evaluated independently. The number of invaded blood vessels was quantified by counting vessels in arbitrary 10 fields of histological sections of porous part of DHC or IBG.

Statistical Analysis

Compressive strength was compared between the porous and solid parts of the DHC implants, using Student's t-test. $p < 0.05$ was considered significant.

RESULTS

Mechanical Compression Test

The compressive strength of the porous (inner) part of the DHC was 12.6 ± 0.4 Mpa, which is comparable to the compressive strength of cancellous bone. In contrast, the compressive strength of the solid (outer) part was 571.8 ± 66.7 Mpa, which is equal to or greater than the compressive strength of cortical bone. The strength of the outer part of the composite was more than 50-fold greater than that of the inner part, and the difference was statistically significant. The breaking load of the DHC implant was 9.6 ± 0.3 kN.

Radiographic Evaluation

In the DHC group, the radiolucent line between the implant and host bone faded with time, but on the cranial side of the implant, the radiodensity between the implant and host bone remained low, compared with other boundaries. None of the implants were found to have collapsed. In the IBG group, all caudal and cranial junctions appeared to have fused with host bone on radiographs. In both groups, the height of the intervertebral space remained constant throughout the follow-up period (Figure 3, Table I).

Micro-Focus CT Evaluation

In the DHC group, the plain radiographic findings correlated well with the CT findings. In all caudal junctions of the DHC group, trabecular bone extended from the host bone and spread to the porous part of the composites. However, on the cranial side of the implant, none of the specimens contained bridging trabecular bone between the implant and host bone. One specimen had a nondisplaced crack line through the inner part of the implant [Figure 4(A-4)], and another specimen had a small crack at the cranial edge of the implant [Figure 4(A-3)].

In the IBG group, 5 of the 8 junctions were bony fused, and the remaining 3 junctions (which were initially judged to be bony fused, based on X-ray findings) were classified as nonbony fused junctions, based on micro-focus CT findings. All of the nonbony fused junctions were on the cranial side of the graft bone (Figure 4, Table I).

Histology

The macroscopic appearance of the histological sections was consistent with the findings of micro-focus CT. In the DHC group, all caudal junctions were found to contain trabecular bone and blood vessels that had spread from host bone into the porous part of the implants [Figure 5(A1–A4,c)]. At the center of each implant, nearly all pores were completely filled with trabecular bone and hematopoietic marrow, including the region that originally contained the vertebral disc [Figure 5(b)]. On the cranial side of the implant, a good portion of the initial gap between the implant and host bone was filled with a fibrocartilage tissue, rather than mineralized bone matrix [Figure 5(a)].

In the IBG group, the caudal side of each graft was bony fused in large part, and it was impossible to identify a boundary between host and graft bone.

The cranial side of 1 of the 4 grafts was mostly bony fused, but in the other 3 samples, there was a thin layer of cartilage tissue between host and graft bone [Figure 5(B)]. Solid part

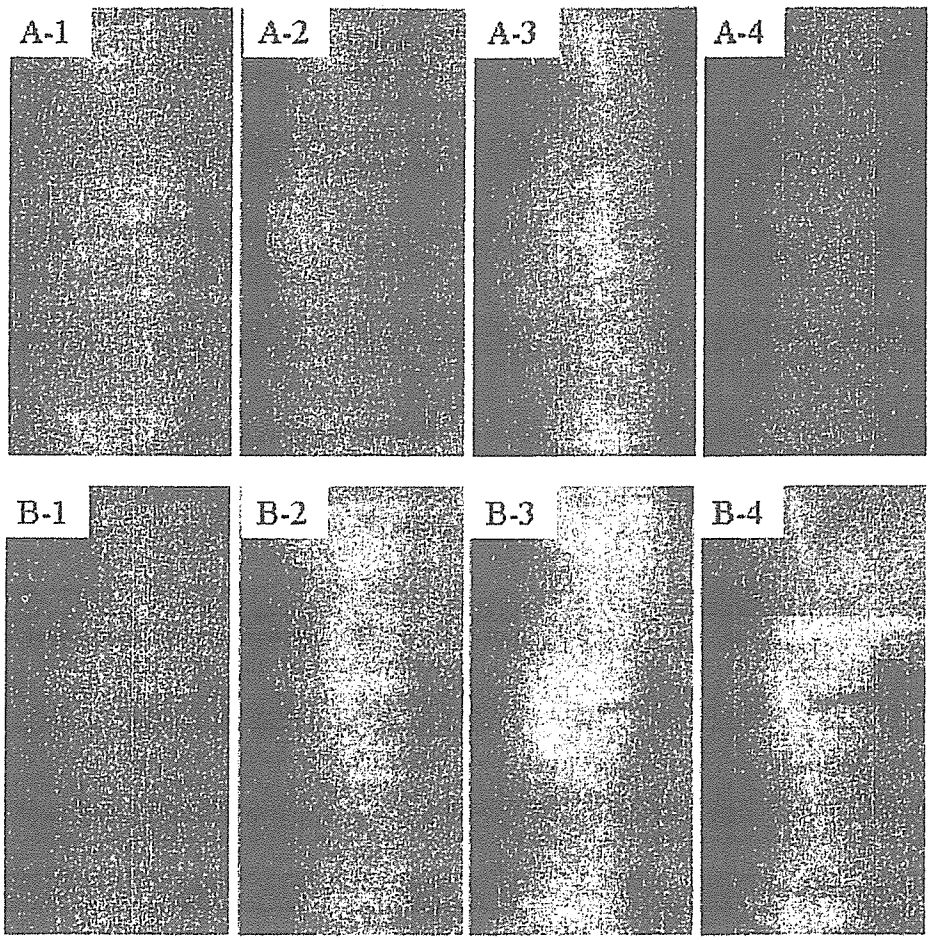

Figure 3. Soft X-ray radiographs. DHC group 6 months after operation (A1–A4). IBG group 6 months after implantation (B1–B4). In both groups, radiopaque shadows were observed at caudal junctional sites. Cranial junctions of DHC group had lower radiodensity than other boundaries between DHC and host bone (A1–A4). Both cranial and caudal sides of all IBG specimens appeared to be radiographically fused (B1–B4).

of the DHC showed by far lower fusion rate when compared with porous part of DHC and IBG.

There was no difference in the invasion of the material by blood vessels between IBG and DHC group.(Figures 6 and 7, Table II).

DISCUSSION

Because of problems including graft extrusion and collapse in animal models and clinical study, HA spinal interbody fusion implants are generally considered unsuitable for clinical applications, despite their high affinity with host bone and their biocompatibility.[4,13,14] Among currently existing porous HA-based bone substitutes, IP-CHA and coralline HA have highly interconnected porous structure with average interconnection channel diameter of 40–60 μm. Those materials have been reported to show excellent bone ingrowth in the materials but their initial compressive strengths are no more than 12 MPa, which is far less than human cortical bone. A porous HA bone substitute with lowest porosity (40%) accomplished the greatest compressive strength of 60 MPa at the sacrifice of osteoconduction but the strength is not still comparable to cortical bone. Our novel dual HA implant (DHC) has well-organized, interconnected, highly porous structure in the porous part and durability under high loads at the same time. In our development of a HA implant for use in spinal interbody fusion, rather than use a material of homogenous composition, we created a composite HA material consisting of two parts with different porosities to produce an implant that combines strength with bone conduction. The outer solid part of the composite (0% porosity), which can chemically bond

TABLE I. Summary of Radiographic Evaluation

	X-ray Evaluation		Micro-Focus CT Evaluation			
					Crack	
Groups	Fusion	Fusion Rate (%)	Fusion	Fusion Rate (%)	Partial	Whole Length
DHC	4/8	50	4/8	50	1/4	1/4
IBG	8/8	100	5/8	62.5		

Each implants or grafts has two junctions between host bone. These data shows union junctions per total junctions (ref. 11).

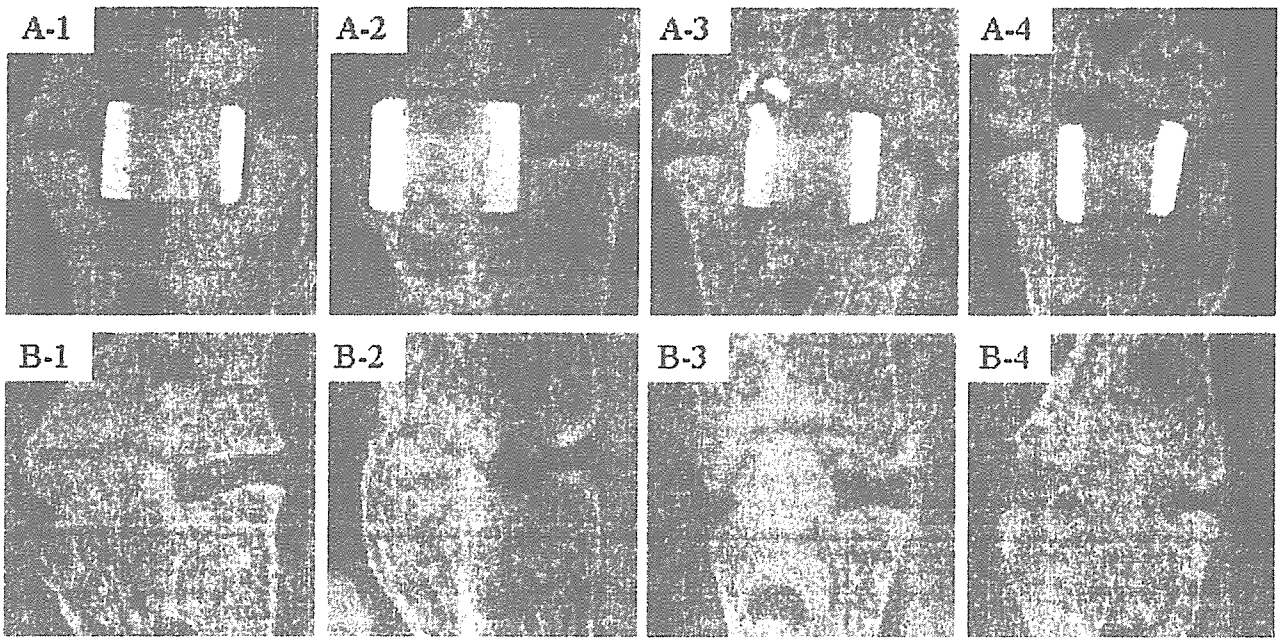

Figure 4. Sagittal reconstruction image of operated spine, based on micro-focus CT data. DHC group 6 months after operation (A1–A4). IBG group 6 months after implantation (B1–B4). In both groups, the caudal side of all junctions was bony fused (A1–A4, B1–B4). Only one sample of the IBG group exhibited osseous union at the cranial junction (B2). At other cranial junctions of both groups, we did not observe bridging trabecular bone between the implant and host bone (A1–A4, B1, B3, B4).

with host bone, is mainly responsible for load bearing, which is the role normally played by cortical bone. The inner porous part of the composite (75% porosity) assumes the role of scaffold to facilitate integration with host bone and thus further strengthen the repair structure.

In the present study, the junctional bony union rate of DHC was 50% and was less than that of the iliac bone grafts. However, most of the junctional gap without bony union was filled with fibro-cartilageous tissue and seemed to be stabilized. Also, only one specimen from the DHC group exhibited a nondisplaced crack spanning the entire length of the implant. None of the DHC implants exhibited axial collapse at any time during the 6-month experimental period. Implant fragmentation is one of the most frequent complications of porous HA implants for intervertebral fusion. DHC seems to have less fragmentation rate but further study with large number is needed to clarify the rate of complications and the advantage of DHC.

Independent of the junctional bony union, the inner part of DHC exhibited excellent bone ingrowth. By covering the porous HA with nonporous HA, the 3D structure of the porous part was preserved throughout the bone conduction process, providing an excellent scaffold for bone ingrowth. The interconnected highly porous structure of IP-CHA, which has an average interconnection diameter of 40 μm, allows efficient migration of bone-producing cells from pore to pore as well as invasion by vascular vessels, which is essential for new bone formation. The present findings help clarify the importance of a stable 3D scaffold for bone ingrowth. The use of a diamond burr in the present procedure

TABLE II. Summary of Histological Evaluation

	Junctions[a]	Tissue Conduction			
		Vessel[b]	Bone[c]		
Groups	Average Bony-Fusion Rate (%)	Average Number of the Blood Vessels	Cranial	Center	Caudal
Porous part of DHC	48	215	4/4	4/4	4/4
IBG	53	193			
Solid part of DHC	19				

[a] Each implants or grafts has two junctions between host bone. These data shows mean bony union length per total junctional length ($N = 4$).
[b] Total number of invaded blood vessels into porous part of DHC and IBG in arbitrary 10 fields ($N = 4$).
[c] Porous part of DHC was divided into three parts. These data shows bone conducted parts per total DHC implants ($n = 2$).

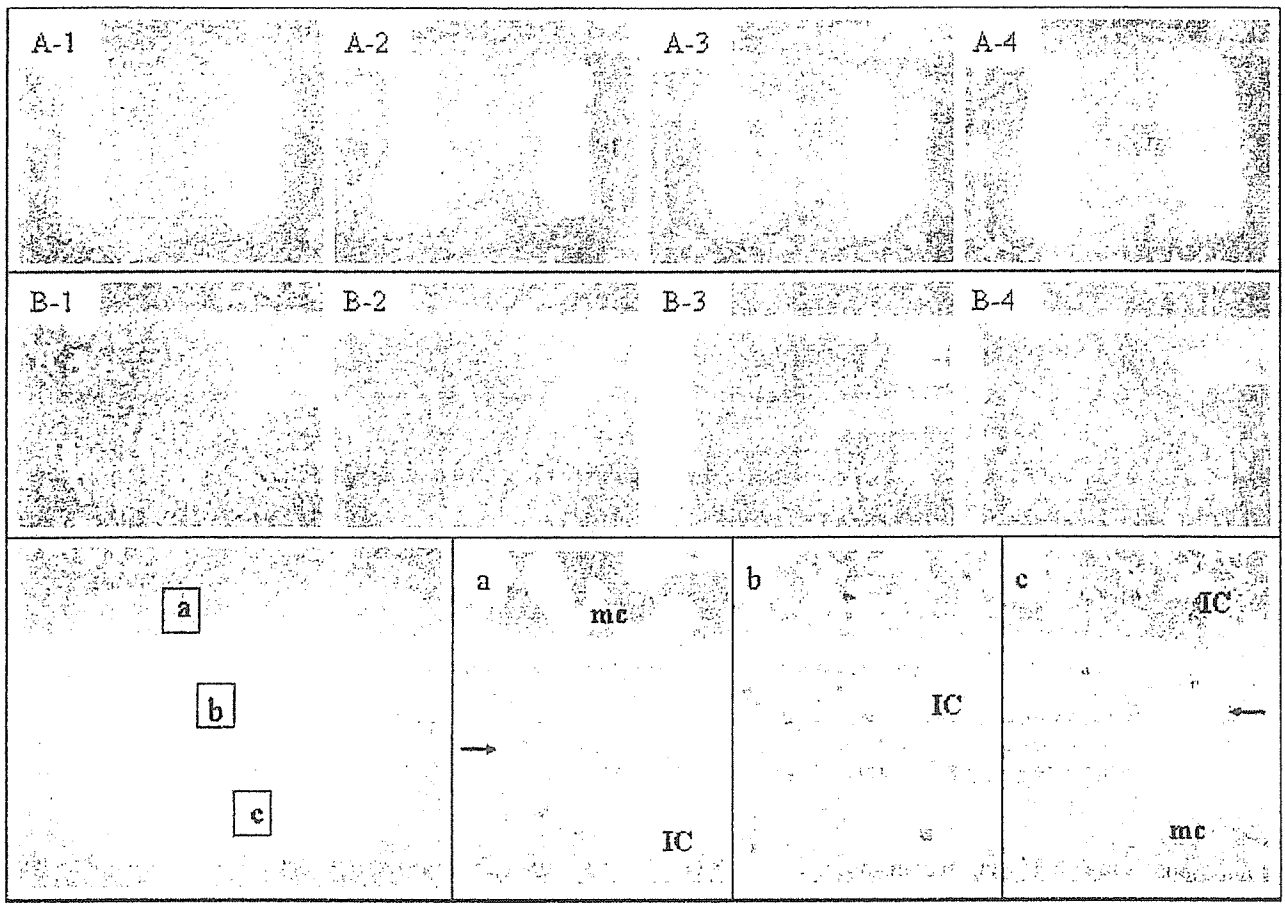

Figure 5. Low-power photomicrographs of operated spines: DHC (A1–A4); and IBG (B1–B4). High-power photomicrographs of DHC group 6 months after operation (a–c). At the cranial side of the implant, we did not observe continuous mineralized trabecular bone between host bone and DHC (a). Almost all pores in the DHC were evenly filled with trabecular bone and hematopoietic marrow (b). At the caudal junction, trabecular bone infiltrated the porous part of DHC, and the gaps were filled with mineralized trabecular bone (c). mc, marrow cavity; IC, IP-CHA. Arrows indicate implant end (magnification: ×40).

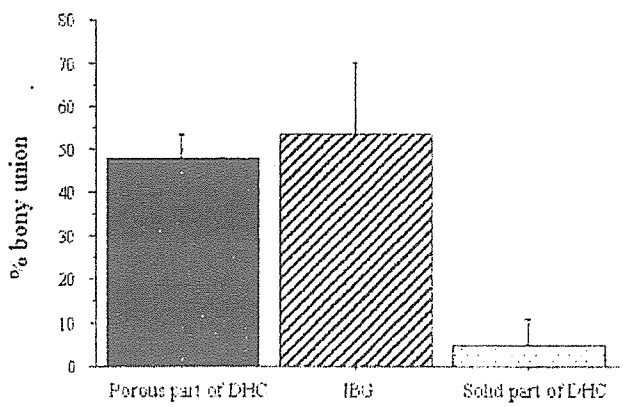

Figure 6. Bone union rates of porous part of DHC, IBG, and solid part of DHC were measured histomorphometrically. Each data bar represents an average and standard deviation ($N = 5$).

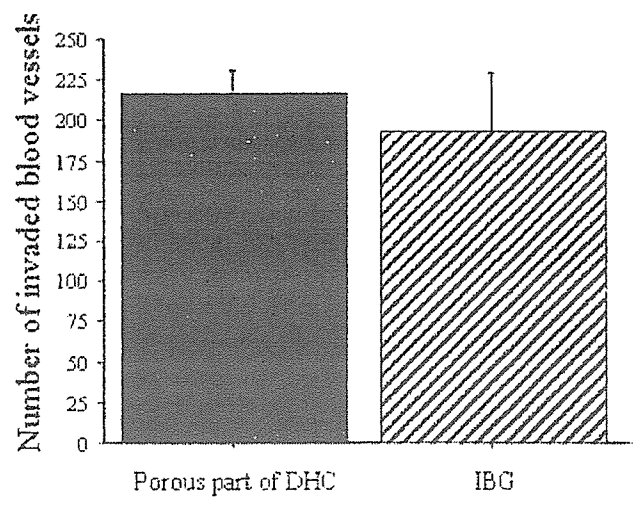

Figure 7. The number of invaded blood vessels were counted in arbitrary 10 fields of histological sections of porous part of DHC or IBG. Each data bar represents an average and standard deviation ($N = 5$).

generates frictional heat, which may have an adverse affect on cell protection and congruency between host bone and implant, and this may inhibit junctional bony union. In terms of their role as scaffolding, interconnected HA and autogenous bone have nearly identical characteristics. In the present animal experiment, the internal fixation at the operative site consisted of a single plate, and was not rigid: no external fixation was applied: and animals were allowed complete freedom of movement immediately after the surgery. However, none of the animals experienced major implant-related complications such as implant collapse, displacement, dislocation, or spinal palsy. Although we observed minor cracks (which did not affect the stability of the implanted sites), our results suggest that DHC has sufficient compressive strength to endure typical intervertebral mechanical loads. The high compressive strength of DHC and the excellent bone ingrowth into the porous part of DHC observed in the present experiment indicate that DHC is highly suitable as a spacing implant material for intervertebral fusion.

However, autogenous bone has the advantage of containing bone-producing cells and several cytokines that contribute to bone induction. HA is an osteoconductive material, but it must be combined with bone-growth-inducing cytokines or bone-producing cells before it can provide results comparable to those of autogenous bone grafts. As we reported previously, porous HA can exhibit good bone-growth-inducing characteristics when it is combined with a cytokine delivery system[15–20] or bone-producing cells such as mesenchymal stem cells. DHC supplemented with those cytokines and cells would be an excellent interbody fusion biomaterial, due to the combination of bone-growth-inducing characteristics and mechanical strength, and it would be a viable substitute for autografts.

CONCLUSIONS

The present findings demonstrate that DHC produces bony fusion that is comparable to that of autogenous iliac bone graft, with strength that is sufficient to withstand normal compressive loads. Further improvement of this material, including incorporation of bone-growth-inducing agents, will increase its usefulness for clinical applications.

We thank Toshiba Ceramics Co., Ltd., for kindly donating implants.

REFERENCES

1. Buttermann GR, Glazer PA, Bradford DS. The use of bone allografts in the spine. Clin Orthop Relat Res 1996;324:75–85.
2. Malloy KM, Hilibrand AS. Autograft versus allograft in degenerative cervical disease. Clin Orthop Relat Res 2002;394:27–38.
3. Blumenthal SL, Ohnmeiss DD. Intervertebral cages for degenerative spinal diseases. Spine J 2003;3:301–309.
4. Goldberg VM. Natural history of autografts and allografts. In: Older J, editor. Bone Implant Grafting. London: Springer-Verlag; 1992. p 9–12.
5. Bucholz RW, Carlton A, Holmes RE. Hydroxyapatite and tricalcium phosphate boe graft substitutes. Orthop Clin North Am 1987;18:323–334.
6. Flatley TJ, Lynch KL, Benson M. Tissue response to implant s of calcium phosphate ceramic in the rabbit spine. Clin Orthop 1983;179:246–252.
7. Ylinen P, Kinnunen J, Laasonen EM, Lamminen A, Vainionpaa S, Raekollio M, Rokkanen P. Lumbar spine interbody fusion with reinforced hydroxyapatite implants. Arch Orthop Trauma Surg 1991;110:250–256.
8. Jeffrey MS. Use of hydroxyapatite in spine surgery. Eur Spine J 2001;10:S197–S204.
9. Emery SE, Fuller DA, Stevenson S. Ceramic anterior spinal fusion. Biologic and biomechanical comparison in a canine model. Spine 1996;21:2713–2719.
10. Lu WW, Zhao F, Luk KDK, Yin YJ, Cheung KMC, Cheng GX, Yao KD, Leong JCY. Controllable porosity hydroxyapatite ceramics as spine cage: Fabrication and properties evaluation. J Mater Sci Mater Med 2003;14:1039–1046.
11. Frank AP, Dennis JM, James PH, Narayon Y, Kark WD, John MR, Brian C. Fusion rate and biomechanical stiffness of hydroxylapatite versus autogenous bone grafts for anterior discectomy. Spine 1994;19:2524–2528.
12. Tamai N, Myoui A, Tomita T, Nakase T, Tanaka J, Ochi T, Yoshikawa H. Novel Hydroxyapatite ceramics with an interconnective porpus structure exhibit superior osteoconduction in vivo. J Biomed Mater Res 2002;59:110–117.
13. Ito M, Abumi K, Shono Y, Kotani Y, Minami A, Kaneda K. Complications related to hydroxyapatite vertebral spacer in anterior cervical spine surgery. Spine 2002;27:428–431.
14. McConnell JR, Freeman BJ, Debnath UK, Grevitt MP, Prince HG, Webb JK. A prospective randomized comparison of coralline hydroxyapatite with autograft in cervical interbody fusion. Spine 2003;28:317–323.
15. Saito N, Takaoka K. New synthetic biodegradable polymers as BMP carriers for bone tissue engineering. Biomaterials 2003; 24:2287–2293.
16. Miyamoto S, Takaoka K, Okada T, Yoshikawa H, Hashimoto J, Suzuki S, Ono K. Evaluation of polylactic acid homopolymers as carriers for bone morphogenetic protein. Clin Orthop 1992; 278:274–285.
17. Miyamoto S, Takaoka K, Okada T, Yoshikawa H, Hashimoto J, Suzuki S, Ono K. Polylactic acid–polyethylene glycol block copolymer: A new biodegradable synthetic carrier for bone morphogenetic protein. Clin Orthop 1993;294:333–343
18. Saito N, Okada T, Horiuchi H, Murakami N, Takahashi J, Nawata M, Ota H, Nozaki K, Takaoka K. A biodegradable polymer as a cytokine delivery system for inducing bone formation. Nat Biotechnol 2001;19:332–335.
19. Kaito T, Myoui A, Takaoka K, Saito N, Nishikawa M, Tamai N, Ohgushi H, Yoshikawa H. Potentiation of the activity of bone morphogenetic protein-2 in bone regeneration by a PLA-PEG/hydroxyapatite composite. Biomaterials 2005;26:73–79.
20. Nishikawa M, Myoui A, Ohgushi H, Ikeuchi M, Tamai N, Yoshikawa H. Bone tissue engineering using novel interconnected porous hydroxyapatite ceramics combined with marrow mesenchymal cells: Quantitative and three-dimensional image analysis. Cell Transplant 2004;13:367–376.

Hydroxyapatite Augmentation for Bone Atrophy in Total Ankle Replacement in Rheumatoid Arthritis

Kenrin Shi, MD, PhD,[1] Kenji Hayashida, MD, PhD,[2] Jun Hashimoto, MD, PhD,[3] Kazuomi Sugamoto, MD, PhD,[4] Hideo Kawai, MD, PhD,[5] and Hideki Yoshikawa, MD, PhD[6]

Although total ankle replacement is routinely used for rheumatoid arthritis of the ankle, it has been hampered by early implant failures such as loosening and subsidence of the tibial component due to poor bone quality. To prevent this complication, total ankle replacement augmented by a specially designed hydroxyapatite coating was used in 14 patients (16 feet). Patients were reviewed after an average follow-up of 23.1 months, and the mean clinical rating scale significantly improved from 30.7/100 points preoperatively to 65.9/100 at final follow-up, especially with respect to pain relief. Radiographs taken immediately postoperatively and at final follow-up were analyzed for the position and sinking of the tibial component. The position was evaluated by measurement of the alpha and beta angles, formed by the tibial long axis and tibial component on anteroposterior and lateral radiographs, respectively. The mean alpha and beta angles were 87.4° and 79.3° postoperatively and 87.7° and 81.0° at final follow-up, respectively. No significant change was noted in either angle between the immediate postoperative views and at final follow-up, and no significant subsidence was noted. Radiographs were also assessed for the presence of a lucent zone: 1 case demonstrated a clear zone between hydroxyapatite and bone, 9 cases between hydroxyapatite and the tibial component, and 6 cases between the tibial component and bone. These results suggest that hydroxyapatite helps to secure implant fixation firmly to the bone, making it a useful augmentation for tibial bone atrophy in total ankle replacement for rheumatoid arthritis. (The Journal of Foot & Ankle Surgery 45(5):308–315, 2006)

Key words: rheumatoid arthritis, total ankle replacement, hydroxyapatite

Arthritic involvement of ankle joint is often observed in patients with rheumatoid arthritis (RA) in middle to late stages of the disease. Michlke et al (1) stated that 52% of 300 patients had presented ankle and subtalar involvement with an average duration of 9.5 years. Because the ankle joint is a weight-bearing joint like the hip and knee, ankle destruction severely impairs standing and walking ability and disturbs a patient's quality of life. Arthrodesis had long been almost the only surgical treatment for this condition before the introduction of total ankle replacement (TAR). However, high nondelayed or delayed union rates after arthrodesis exist, possibly because of poor immunologic and metabolic conditions in patients with RA treated with steroid-type or antimetabolite-type medications (2).

TAR was first introduced in the early 1970s as an alternative to ankle arthrodesis, but high complication rates of early prosthesis designs such as severe osteolysis, component loosening, impingement, infection, and soft tissue breakdown were reported (3). These first-generation TAR prostheses often consisted of 2 components, tibial and talar, with a highly constrained design, and were thought to result in early failure because of the increased force between the bone and implant (4, 5).

The second-generation TAR with a less constrained component design was introduced in the 1980s; some can be fixated without cement and some possess a mobile-bearing (three-component) design. Kofoed and Sorensen reported no significant difference in clinical outcomes in patients with RA versus osteoarthritis (OA) with the use of the cemented Scandinavian Total Ankle Replacement (STAR) prosthesis, one of the second-generation TAR implants (6). These recent successful results have encouraged surgeons to perform TAR instead of arthrodesis, even in RA.

Address correspondence to: Kenrin Shi, MD, 4-8-1 Hoshigaoka, Hirakata, Osaka, 573-8511, Japan. E-mail: kenrin1968@yahoo.co.jp

[1]Staff doctor, Department of Orthopedics, Hoshigaoka Koseinenkin Hospital, Osaka, Japan.

[2]Director, Department of Orthopedics, Hoshigaoka Koseinenkin Hospital, Osaka, Japan.

[3]Assistant professor, Department of Orthopaedic Surgery, Osaka University Medical School, Osaka, Japan.

[4]Associate professor, Department of Orthopaedic Surgery, Osaka University Medical School, Osaka, Japan.

[5]Vice president, Department of Orthopedics, Hoshigaoka Koseinenkin Hospital, Osaka, Japan.

[6]Professor and chairman, Department of Orthopaedic Surgery, Osaka University Medical School, Osaka, Japan.

1067-2516/06/4505-0001$32.00/0
doi:10.1053/j.jfas.2006.06.001

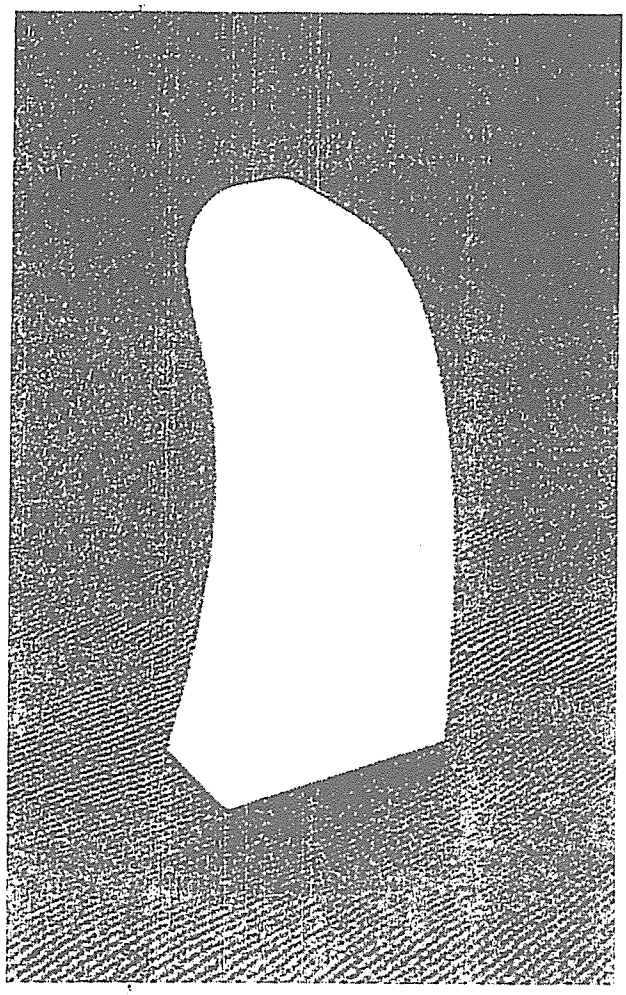

FIGURE 1 HA used in this study for tibial augmentation.

Although TAR has been performed in patients with RA increasingly in this decade, and favorable clinical outcomes with significant pain relief have been achieved, early implant failure such as loosening and subsidence of the implants is still a problem, often because of poor bone quality of the implanted site (4). As an attempt to solve this problem, especially in fixation of the tibial component, we used a specifically designed hydroxyapatite (HA) to augment the tibial bone atrophy in conjunction with TAR for rheumatoid ankles. The purpose of this article is to report the short-term outcomes and radiographic findings of this procedure.

Materials and Methods

HA (Bonecеram; Olympus Biomaterial Corp., Tokyo, Japan) was designed and formed such that it could be inserted into the tibia easily, but would fit within the inner cortex of the distal tibia (Fig 1). The sizes of the HA component were determined according to previously obtained data of the transverse and sagittal diameter of the inner cortex of the distal tibia on anteroposterior (AP) and lateral radiographs of patients with RA (K. S., unpublished data, 1999).

Outcomes were evaluated clinically and radiographically. Clinically, each ankle was scored according to a rating scale created by Takakura et al (7), which includes an assessment of pain relief as well as functional improvement such as walking ability, the ability to climb stairs, and range of motion (Table 1). The physical examination and patient interview were conducted by each surgeon preoperatively, but by the first author (K. S.) at final follow-up. Scores rated before the surgery and at the last follow-up were compared

TABLE 1 Clinical rating scale

Pain	
None	40
Mild	30
Moderate	20
Severe	10
Disabled	0
Function	
Walking distance	
Unlimited	20
2 km	15
0.5–2 km	10
Indoors only	5
Unable to walk	0
Limping	
None	4
Moderate	2
Unable to walk	0
Stairs (up)	
Normally	4
Needs banister	2
Unable	0
Stairs (down)	
Normally	4
Needs banister	2
Unable	0
Standing on operated leg	
Normally	4
Needs support	2
Unable	0
Sitting Japanese style	
Normally	4
Easy posture	2
Unable	0
Dorsiflexion	
11°–	10
6°–10°	7
1°–5°	4
0°	0
Plantarflexion	
36°–	10
21°–35°	7
6°–20°	4
5°	0

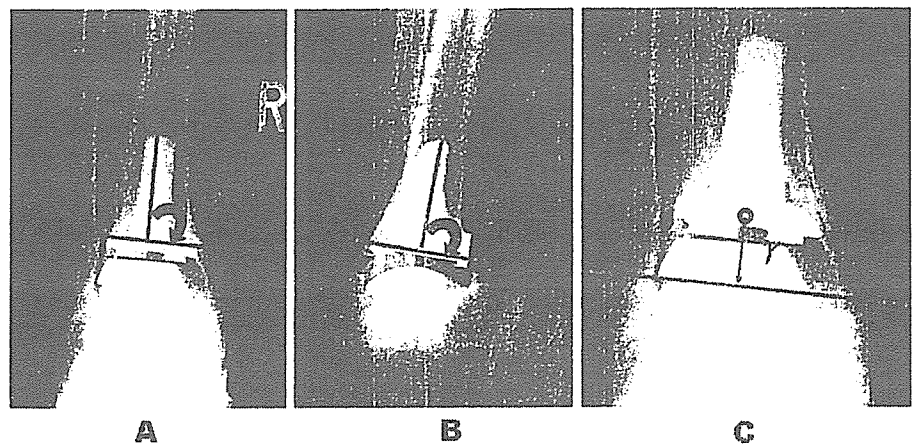

FIGURE 2 Radiographic evaluation of placement and subsidence of the tibial component. (*A*) Alpha angle. (*B*) Beta angle. (*C*) Gamma length.

and statistically examined by Wilcoxon signed-rank test. *P* values $<.05$ were considered to be significant.

AP and lateral radiographs taken immediately postoperatively and at final follow-up were compared with respect to the placement and migration of the tibial component. Placement was assessed with 2 angles: 1) the alpha angle, formed by the long axis of the tibia and the transverse line of the tibial component on the AP radiograph (Fig 2, A); and 2) the beta angle, formed by the long axis of the tibia and the sagittal line of the tibial component on lateral radiographs (Fig 2, B). Subsidence was evaluated by the following measurement on AP radiographs. First, a baseline that crossed the most prominent part of medial malleolus was determined perpendicular to the tibial long axis. Then, the length from the center of the tibial component to the baseline was measured and defined as the gamma length (Fig 2, C). Finally, the clear zone, determined as the radiolucent zone around the implant with a width ≥ 1 mm, was also assessed on AP radiographs as an indication of early loosening, either between the HA and the bone, HA and the tibial component, or the tibial component and bone. These radiographic data were obtained solely by the first author (K. S.), independent from the operating surgeons. Data obtained from radiographs taken immediately postoperatively and at the last follow-up were compared and statistically examined by use of Wilcoxon signed-rank test, with *P* values $<.05$ recognized as significant.

Surgical Technique

All procedures were performed through an anterior approach. After bone resection from the distal tibia, retrograde intramedullary rasping was performed to allow insertion of the HA. Then the HA was inserted into the tibia from the inferior aspect of the tibia, with its apex directed proximally and anteriorly. A TNK implant (Japan Medical Materials Corporation, Osaka, Japan) was used in all cases except 1, in which a FINE (Nakashima Medical, Okayama, Japan) was used. The TNK uses ceramic components with polyethylene on a tibial-bearing surface (8), whereas the FINE consists of metal tibial and talar components with a polyethylene mobile bearing between the components (9). All implants were fixated with bone cement. Concurrent subtalar joint arthrodesis was performed in 11 ankles that demonstrated subtalar deformity, erosion, and/or instability. All procedures were performed by one of 3 senior authors (K. H., J. H., K. Su.).

Ankles without subtalar arthrodesis were immobilized in a soft splint for 3 weeks, and then range-of-motion exercises and full weight bearing were started. Ankles with subtalar arthrodesis were immobilized in a short leg cast for 4 to 6 weeks, and full weight bearing was permitted 10 weeks postoperatively.

Results

Sixteen ankles (14 patients) were studied with a mean follow-up period of 23.1 months (range, 7–73 months). Two patients were men and 12 were women. Two patients underwent surgery on bilateral ankles separately. The mean patient age was 61.4 years (range, 48–74 years).

Clinical rating scale scores improved from 30.7 points (range, 14–42) preoperatively to 65.9 points (range, 27–86) at final follow-up (Fig 3).

Radiographic measurements are shown in Table 2. The mean alpha angle was 87.4° (range, 82.5–95°) postoperatively and 87.7° (range, 81.5–97°) at final follow-up. The mean beta angle was 79.3° (range, 72–89°) and 81.0° (range, 49–102°), respectively. The change in each angle from immediately postoperatively to the time of final follow-up was not found to be significant. The mean gamma length was 11.8 mm (range, 7–19 mm) postoperatively and 12.0 mm (range, 7.5–20 mm) at final follow-up, and no significant difference was found between these values. The

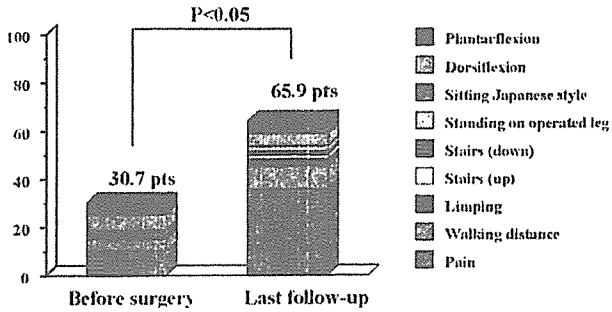

FIGURE 3 Clinical rating scale scores before surgery and at last follow-up.

TABLE 2 Results of radiographic evaluation of tibial component

	Postoperative	Last Follow-Up	*P* Value
Alpha angle	87.4	87.7	NS
Beta angle	79.3	81	NS
Gamma length (mm)	11.8	12	NS

Abbreviation: NS, not significant.

mean amount of sinking, defined as the increase of gamma length, was 0.2 mm.

One ankle demonstrated a clear zone between the HA and bone, 9 exhibited a clear zone between HA and the tibial component (Fig 4), and 6 demonstrated a clear zone between the tibial component and bone. Two ankles demonstrated early loosening, recognized as implant migration on radiographs. One of these underwent revision 6 months after the primary surgery (Fig 5). No clear zone was observed between HA and bone in either of these 2 cases. In the ankle that underwent revision, firm fixation between HA and bone was confirmed during the revision surgery.

Discussion

The first-generation TAR, introduced in the 1970s, resulted in high complication rates and early failures because of increased force between the bone and implant due to their highly constrained design (3–5). The second-generation TAR, introduced in the 1980s, has a less constrained design and, so far, has been used with favorable clinical results (6). Anderson et al (10) also reported a similar revision and loosening rate in patients with RA and OA after uncemented STAR prosthesis, with an estimated 5-year survival rate of 70%, with revision as the end point. Another second-generation TAR was reported to present a 5-year survival rate of 54%, in a study of mostly relatively young patients with posttraumatic or primary OA (11).

However, even in such prostheses with advanced designs,

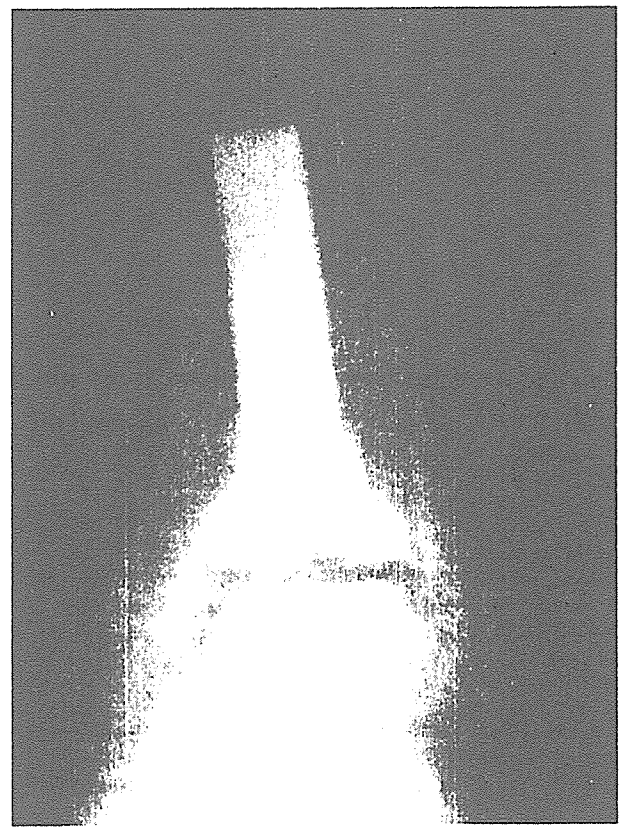

FIGURE 4 AP radiograph demonstrating a clear zone between HA and the tibial component. In this case, a clear zone between HA and the tibial component was obvious, whereas no clear zone was recognized between HA and bone or between bone and the tibial component.

arthritic involvement and deformity in hindfoot and other major lower extremity joints can lead to early failure of the ankle prosthesis in patients with RA (12). Kofoed and Sorensen reported that a progression of hindfoot valgus deformity resulted in failure of TAR in patients with RA (6). A radiographic evaluation of the ankle and subtalar joint of patients with RA has also shown that subtalar pathology precedes changes in the ankle joint in the natural course of RA (13). For this reason, the authors performed corrective arthrodesis of subtalar joint not only in patients with an existing subtalar deformity, but also in those demonstrating subtalar erosion and/or instability that would be expected to cause valgus deformity or pain.

Another issue contributing to early failure in TAR in RA is implant migration due to poor bone quality. Of the 12 revisions in the report by Anderson et al (10), the reason for revision was loosening of the tibial component in 2 patients, the talar component in 2 patients, and both components in 3 patients. Carlsson et al (14) also reported a similar migration pattern of tibial and talar components of the STAR prosthe-

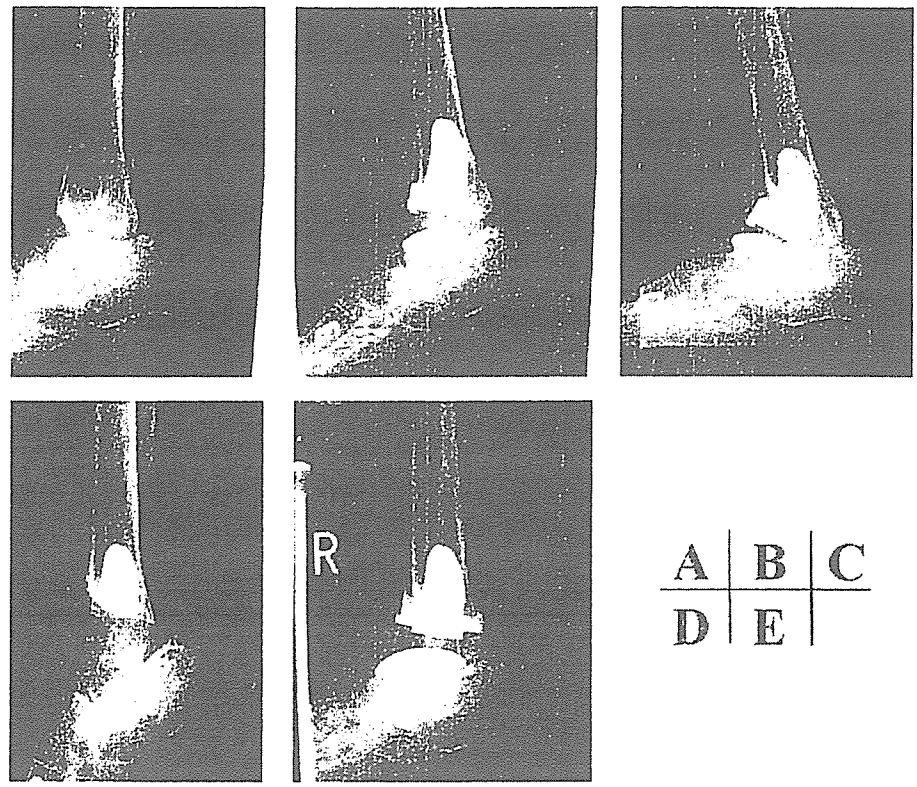

FIGURE 5 A case of a 64 year-old woman who demonstrated early loosening that necessitated a revision surgery 5 months after the initial surgery. However, no clear zone was observed between HA and bone on radiographs, and firm fixation between HA and the implanted site was confirmed during the revision surgery. (*A*) Before surgery. (*B*) After the initial surgery. (*C*) Loosening of the tibial component was noted. (*D*) Firm bonding of HA with the implanted site bone was noted after removal of the tibial component. (*E*) After the revision surgery.

sis after 3 to 5 years of follow-up. On the other hand, Su et al (15) reported that 3 of 26 ankles presented subsidence of the tibial component after an uncemented TAR. In this study, HA was only used for augmentation of tibial bone atrophy, partly because subtalar arthrodesis was performed in many cases, preventing the bulk augmentation of the talus in those cases.

Over the last 2 decades, HA has been used to augment bone loss more in facial and dental surgery than orthopedic surgery because of concern about its ability to withstand weight-bearing forces (16, 17). However, clinical reports of HA used for spine surgery (18) and revision total hip arthroplasty (19) have encouraged its use in lower extremity surgery. As for the HA used in this study, Itokazu and Matsunaga (20) reported the use of this material as a graft in bone defect in the treatment of tibial plateau fractures. Koshino et al (21) used a wedge-shaped block of Boneceram in a medial open-wedge proximal tibial ostotomy for knee OA without collapse or subsidence.

The results of the current study show that the position of the tibial implant was secured without migration in most cases, and this compound could be helpful in securing the initial placement of the implant. Neither breakage nor collapse of HA was observed. In addition, firm bonding with the bone was demonstrated radiographically in most cases and intraoperatively in 1 case during the revision surgery. Although histological examination was not performed in this case, a previous study has shown incorporation into the surrounding bone (20). Therefore, this material provides an option for augmentation of tibial bone atrophy in TAR in patients with RA.

HA is now also used in several types of cementless TAR as a coating material over metal implants similar to other joint prostheses, to promote firm bonding between the bone and implant. Bonnin et al reported decreased radiolucency with the use of the Salto prosthesis (Tornier SA, Saint Ismier, France) with HA coating (22). Kofoed reported a longer survival rate of cementless HA-coated STAR prosthesis (Waldemar Link, Hamburg, Germany) as compared with a cemented implant at a mean 12 years postoperatively (23). Moreover, a double-coated prosthesis, coated with 300 μm plus 25 μm thickness of HA, has recently been introduced (24). Its radiostereometric analysis demonstrated initial migration of both tibial and talar components at 6 weeks without progression or bone resorption, and there was no difference in these results between patients with RA and OA (14). In addition to bulk augmentation as it was used in this study, HA may also be a promising agent for implant fixation in TAR.

The results of this study do demonstrate one major concern: the high frequency of radiolucency. More than half of the ankles studied demonstrated a clear zone between HA and

the tibial component on radiographs at the final follow-up. Two ankles resulted in radiographic loosening recognized as implant migration, one of which required revision. Although firm bonding between HA and bone was recognized, a certain limitation remains, in that cement fixation between HA and the implant was unsatisfactory. Perhaps the amount of pressurization during solidification of bone cement may not have been adequate.

In conclusion, the HA presented in this study provides an option for augmentation of tibial bone atrophy in TAR for patients with RA, because it bonded firmly to bone at the implantion site. Migration or subsidence of the tibial implant was not observed in most cases. Methods for firm fixation of implants with HA should be developed, and bonding of HA with bone should be scrutinized over a longer-term follow-up.

References

1. Michlke W, Gschwend N, Rippstein P, Simmen BR. Compression arthrodesis of the rheumatoid ankle and hindfoot. Clin Orthop 340: 75–86, 1997.
2. Nassar J, Cracchiolo A 3rd. Complications in surgery of the foot and ankle in patients with rheumatoid arthritis. Clin Orthop Relat Res Oct;140–152, 2001.
3. Bolton-Maggs BG, Sudlow RA, Freeman MAR. Total ankle arthroplasty. A long-term review of the London Hospital experience. J Bone Joint Surg Br 67:788–790, 1985.
4. Coutu SF, Wong YS. Complications of total ankle replacement. Clin Orthop 391:105–114, 2001.
5. Easley MD, Vertullo CJ, Urban WC, Nunley JA. Perspectives on modern orthopaedics. Total ankle arthroplasty. J Am Acad Orthop Surg 10:157–167, 2002.
6. Kofoed H, Sorensen TS. Ankle arthroplasty for rheumatoid arthritis and osteoarthritis. Prospective long term study of cemented replacement. J Bone Joint Surg Br 80:328–332, 1988.
7. Takakura Y, Tanaka Y, Sugimoto K, Tamai S, Masuhara K. Ankle arthroplasty. A comparative study of cemented metal and uncemented ceramic prostheses. Clin Orthop 252:209–216, 1990.
8. Takakura Y, Tanaka Y, Kumai T, Sugimoto K, Ohgushi H. Ankle arthroplasty using three generations of metal and ceramic prostheses. Clin Orthop 424:130–136, 2004.
9. Nakashima Medical. Available at: http://www.nakashima.co.jp/Medical/product/ashi.html. Accessed December 20, 2005.
10. Anderson T, Montgomery F, Carlsson A. Uncemented STAR total ankle prostheses. Three to eight-year follow-up of fifty-one consecutive ankles. J Bone Joint Surg Am 85:1321–1329, 2003.
11. Spirt AA, Assal M, Hansen ST Jr. Complications and failure after total ankle arthroplasty. J Bone Joint Surg Am 86:1172–1178, 2004.
12. Felix NA, Kitaoka HB. Ankle arthrodesis in patients with rheumatoid arthritis. Clin Orthop 349:43–47, 1998.
13. Belt EA, Kaarela K, Maenpaa H, Kauppi MJ, Lehtinen JT, Lehto MU. Relationship of ankle joint involvement with subtalar destruction in patients with rheumatoid arthritis. A 20-year follow-up study. Joint Bone Spine 68:154–157, 2001.
14. Carlsson A, Markusson P, Sundberg M. Radiostereometric analysis of the double-coated STAR total ankle prosthesis: a 3–5 year follow-up of 5 cases with rheumatoid arthritis and 5 cases with osteoarthrotis. Acta Orthop 76:573–579, 2005.
15. Su EP, Kahn B, Figgie MP. Total ankle replacement in patients with rheumatoid arthritis. Clin Orthop 424:32–38, 2004.
16. Jarcho M. Retrospective analysis of hydroxyapatite development for oral implant applications. Dent Clin North Am 36:19–26, 1992.
17. Zeltser C, Masella R, Cholewa J, Mercier P. Surgical and prosthodontic residual ridge reconstruction with hydroxyapatite. J Prosthet Dent 62:441–448, 1989.
18. Spivak JM, Hasharoni A. Use of hydroxyapatite in spine surgery. Eur Spine J 10:S197–S204, 2001.
19. Oonishi H, Iwaki Y, Kin N, Kushitani S, Murata N, Wakitani S, Imoto K. Hydroxyapatite in revision of total hip replacements with massive acetabular defects: 4- to 10-year clinical results. J Bone Joint Surg Br 79:87–92, 1997.
20. Itokazu M, Matsunaga T. Arthroscopic restoration of depressed tibial plateau fractures using bone and hydroxyapatite grafts. Arthroscopy 9:103–108, 1993.
21. Koshino T, Murase T, Saito T. Medial opening-wedge high tibial osteotomy with use of porous hydroxyapatite to treat medial compartment osteoarthritis of the knee. J Bone Joint Surg Am 85:78–83, 2003.
22. Bonnin M, Judet T, Colombier JA, Buscayret F, Graveleau N, Piriou P. Midterm results of the Salto Total Ankle Prosthesis. Clin Orthop 424:6–18, 2004.
23. Kofoed H. Scandinavian Total Ankle Replacement (STAR). Clin Orthop 424:73–79, 2004.
24. Anderson T, Montgomery F, Carlsson A. Uncemented STAR total ankle prostheses. J Bone Joint Surg Am 86tsuppl 1):103–111, 2004.

Ⅳ－Ⅱ　分担研究刊行物

B）重症化機序解明と治療法開発研究

1）ナース細胞（線維芽細胞様細胞）病態解析研究
①未分化骨髄からのナース細胞分化機序解明研究
②滑膜細胞の病理学的特性解析研究

2）骨吸収機序解析研究
①骨吸収の病態解析研究
②遺伝子改変マウスによるRA患者のMMP12遺伝子病態解析研究
③RANKL依存性破骨細胞におけるRANKL切断活性の意義
④脂肪組織によるRA特異的破骨細胞抑制効果